PAPER • OPEN ACCESS

Unravelling the role of iron and manganese oxides in colouring Late Antique glass by micro-XANES and micro-XRF spectroscopies

View the article online for updates and enhancements.

Journal of Physics: Photonics

PAPER

Unravelling the role of iron and manganese oxides in colouring Late Antique glass by micro-XANES and micro-XRF spectroscopies

Francesca Gherardi[1,*] ⓘ, Clément Hole[2], Ewan Campbell[3], Marine Cotte[2,4], Rachel Tyson[5] and Sarah Paynter[1]

1 Investigative Science, Historic England, Portsmouth, United Kingdom
2 European Synchrotron Radiation Facility (ESRF), Grenoble, France
3 School of Humanities, University of Glasgow, Glasgow, United Kingdom
4 LAMS, CNRS UMR 8220, Sorbonne Université, UPMC Univ Paris 06, Paris, France
5 Consultant glass specialist, Stroud, United Kingdom
* Author to whom any correspondence should be addressed.

E-mail: Francesca.gherardi@historicengland.org.uk

Keywords: Late Antique glass, XANES, colouring techniques, XRF, manganese, iron redox

Supplementary material for this article is available online

Abstract

This research aims to understand colouring technologies in 5th–7th centuries glass imported to Atlantic Britain by correlating the iron (Fe) and manganese (Mn) ratios and oxidation states with colour. Despite having a similar matrix chemical composition and concentrations of Fe and Mn oxides, these vessels display different colours (from green to yellow/amber, sometimes with purple streaks). Colour changes can be induced by controlling the reduction-oxidation reactions that occur during glass production, which are influenced by the raw materials, furnace and melt atmosphere, and recycling. To evaluate these parameters, reference glasses were prepared, following the composition of Late Antique archaeological glass recovered from Tintagel (UK) and Whithorn (UK). A corpus of archaeological and experimental glass samples was analysed using bulk Fe and Mn K-edge x-ray absorption near edge structure (XANES) spectroscopy, micro-XANES and micro x-ray fluorescence (μ-XRF) at beamline ID21, at the European Synchrotron Radiation Facility. Fe and Mn XANES spectra of the archaeological glass indicate that Fe and Mn are in a similar oxidation state in all the yellow samples, predominantly Fe^{3+} and Mn^{2+}. No detectable difference in Mn and Fe oxidation state occurs in the purple streaks compared to the yellow glass bulk but μ-XRF maps of the distribution of Fe and Mn show that Mn is more concentrated in the purple streaks. This indicates that the purple colour of the streaks is mainly due to a higher Mn/Fe ratio and persistence of more oxidised manganese in the purple areas, even though it is difficult to detect. Many archaeological fragments appear pale green in transmitted light but amber in reflected light. XANES studies detected the presence of surface layers where manganese is more oxidised. This layer is believed to scatter transmitted and reflected light differently and might be responsible for the optical features of the archaeological glass.

1. Introduction

1.1. Background

Although glass was widely used in Roman Britain, it becomes much rarer in the Late Antique period and the vessels have a noticeably different appearance, in both style and colour [1, 2]. The glass itself was made on a vast scale in the form of large slabs at glass manufactories in Egypt and the Levant coast [3–5]. From there the glass slabs were broken up and exported widely to workshops across the Mediterranean and Europe where it was re-melted and made into vessels for further distribution [6].

The key ingredient in this glass was 'natron', a source of sodium-rich minerals that formed in the Wadi Natrun in Egypt [7], which was combined with sand. The colour of natron glass was due largely to iron-rich

impurities in the sand but was commonly modified by adding compounds of antimony or manganese to influence the oxidation state of the iron dissolved in the glass. The redox conditions were further influenced by the melting conditions (temperature, duration and atmosphere of heating) and the degree of recycling, since recycled glass (cullet) would often contain more impurities and have an altered oxidation state relative to freshly made glass [8]. By the Late Antique period, transparent glass usually contains manganese rather than antimony as a colour-modifier [9] and has a stronger green or olive hue relative to Roman glass because the iron content of the glass increases significantly [10].

1.2. Archaeological glass
The archaeological glass studied here is a style characterised as Atlantic tradition glass by Campbell [11–14], which is known from sites along the west coast of Britain and Ireland, and was imported from the Bordeaux region of western France. Atlantic tradition glass is pale yellowish to amber coloured, often decorated with opaque white glass trails (Group C), but may be undecorated (Group D), and in the form of cone beakers or small bowls. Some of these fragments display an amber colour with purple streaks. The glass studied here comes from Tintagel, a high-status settlement on a promontory in the far southwest of Britain, and from Whithorn, in the southwest of Scotland, another high-status settlement which became an important place of Christian pilgrimage in the Late Antique period. A variant of the Atlantic tradition is found at Whithorn, the 'Whithorn' tradition (Group E), and may have been manufactured there. The composition of the glass is a natron type known as Foy 2.1, which is thought to originate in Egypt but has been identified across Continental Europe and the Byzantine Empire, including Cyprus, France, Spain, Italy, Germany, Bulgaria, North Africa, Egypt, and Britain [15–22]. Foy Type 2.1 is noticed particularly in the 6th and 7th centuries AD but is thought to have originated in the late 5th century. It is typically yellow/greenish, but there is also an iron-rich variant, which has a deeper green colour and is mainly noted from the mid-6th century onwards.

1.3. Influence of manganese and iron on natron glass colour
Previous studies have investigated the range of colour in natron glasses [23–25] with a focus on Roman and Late Roman glass of slightly different composition by using X-ray absorption near edge structure (XANES) and optical spectroscopy to characterise the oxidation states of iron and manganese.

The combined presence of iron (Fe) and manganese (Mn) produces glasses with a wide range of colours (from green to amber to purple). In the presence of iron, manganese can either act as a purple colourant when present as Mn^{3+} or can oxidise the bluish reduced iron (Fe^{2+}) to its yellowish oxidised form (Fe^{3+}), resulting in its almost colourless form (Mn^{2+}). The reaction that would occur between Fe and Mn is the following:

$$Fe^{2+} + Mn^{3+} \rightleftharpoons Fe^{3+} + Mn^{2+}. \tag{1}$$

In XANES spectra of iron in glass, the energy position of the pre-edge peak and the main edge have been found to be strongly influenced by the oxidation state (shifted to higher energy for Fe^{3+}). Besides the pre-edge intensity varies as a function of the site symmetry. A shift to higher energy for the pre-edge and the main-edge is also observed at the Mn K-edge with increasing Mn oxidation state [23, 24, 26–29]. However, determining a link between glass colour and Mn speciation (2+, 3+ and 4+) in ancient glass has proved more complex than for iron; whilst distinctions are clear in mineral samples with different oxidation states [30–32], studies of ancient and reproduction glasses have consistently failed to detect much variation in Mn K-edge spectra using XANES in glasses of different colours [23, 28]. Analyses suggest a prevalent presence of the almost colourless Mn^{2+} dominating the XANES spectrum, and possibly hiding the additional presence of the pink Mn^{3+} form, even in strongly purple glass. De Ferri *et al* [23] showed that XANES failed in detecting Mn^{3+} in a Mn^{2+} rich purple glass, while Mn^{3+} is more clearly detected by UV–VIS spectroscopy. One of the advantages of the use of optical absorption spectroscopy is the determination of both Fe and Mn ions simultaneously, although their quantification is problematic due to the difficult assessment of the ions site geometry in glasses [33]. The same observations were made by Schalm *et al* [34] and Arletti *et al* [24], who emphasised that the higher oxidation states of Mn are likely unstable at the temperatures used in glass production. Capobianco *et al* [28] investigated a wide range of flesh-tone to purple glass in medieval stained glass and confirmed that the vast majority (at least 95% of the total Mn) of manganese in the glass is Mn^{2+} and that the remaining small amount of Mn^{3+} shifts the colour from light pink to purple. It was also underlined that purple glass can be produced only in unusually oxidising conditions. As demonstrated in reaction (1), Fe^{2+} and Mn^{3+} cannot be present in glasses at equilibrium, leading to the hypothesis that a short duration of melting and fining is necessary to promote an oxidised redox state of manganese in out of equilibrium conditions. The time taken for melts to reach equilibrium, the influence of pot size and geometry and furnace atmosphere, the addition of reducing agents, and the use of different raw materials are

discussed by Bidegaray *et al* [25] and the impact of some of these issues can also be seen in the experimental melts recreated for this study.

1.4. Aims

The Atlantic tradition glass is visually very distinctive; it is thin, good quality and has an unusual pale yellow to amber colour. Conversely most contemporary glass from Anglo-Saxon sites in Britain and north-western France is more often shades of blue, green or brown, despite being made from the same type of glass [18, 35]. The colour and appearance of the Atlantic tradition glass was intentionally created by the glassworkers and these properties were valued by the communities on the West coast of Britain.

This paper investigates the colouring technologies used by glassworkers in 5th–7th century glass imported to Atlantic Britain by correlating the glass colour with the iron and manganese ratios and their oxidation states. In particular, this study focuses on: (1) the influence of different glass production parameters (addition of reducing and oxidising agents, effects of mixing and re-melting glass batches produced in different redox conditions and changes in melting duration) in experimental glass samples; (2) the variation of Fe and Mn oxidation states in archaeological glass with visible heterogeneity in the form of purple streaks; and (3) the optical character of some of the archaeological samples.

Experimental natron-type glass and archaeological glass from Tintagel and Whithorn (UK) were analysed using different synchrotron-based techniques, including bulk Fe and Mn K-edge XANES spectroscopy, micro-XANES (μ-XANES) and micro X-ray fluorescence (μ-XRF). The Fe and Mn distribution and oxidation states in the samples was mapped by μ-XRF and μ-XANES, respectively.

2. Materials and methods

2.1. Materials

2.1.1. Archaeological glasses

The archaeological glass samples studied here belong to the Atlantic tradition glass and they were recovered from archaeological excavations in Tintagel and Whithorn (UK) (table 1). In some of the archaeological glass, there were visible purple bands, probably from incomplete mixing, which suggested some alteration of the glass colour just prior to blowing the vessels (figure 1). In addition, some Atlantic tradition glass appears pinkish/yellow in reflected light but greener when viewed in transmitted light (figure 1).

2.1.2. Experimental glass

In addition to the archaeological glass samples, a series of experimental glasses with known compositions (following the chemical composition of the archaeological glass from Tintagel and Whithorn) were made up under controlled conditions by glassworkers Mark Taylor and David Hill (table 2 and figure 2). These batches investigated three variables:

(1) Composition: Test glass batches S1 and S2, each 150 g, were melted for 2 h in a gas furnace at 1300 °C in ceramic crucibles with lids. The glass was then cast onto a surface and cooled in air. These batches contained different ratios of iron to manganese oxides (table 2).

(2) Redox: Small test glass batches S1, and S1a–S1d, each 150 g, were melted for 2 h in a gas furnace at 1300 °C in ceramic crucibles with lids. The glass was then cast onto a surface and cooled in air. These batches all had the same composition, S1, but in batches S1a to S1d different amounts of $KC_4H_5O_6$ (a reducing agent) were substituted for K_2CO_3 (table 2).

(3) Mixing: Multiple large batches with composition S1 and S1d were made in a pot without a lid, each 1 kg in total, melted overnight in a gas furnace using a gas/air mix at 1300 °C (renamed P1 and P1d). These were cooled and crushed to chunks of 1 cm or less. These were mixed and remelted (M1 and M2) to create the amber colour of Atlantic tradition glass. M2i contains a higher proportion of P1 to P1d than M1.

(4) Heating duration: The second mixture was heated for a day and sampled after mixing (M2i), after 1 h (M2ii) and after a day (M2iii).

Both the archaeological and experimental glass specimens were mounted in resin and polished to a ¼ micron finish to be analysed.
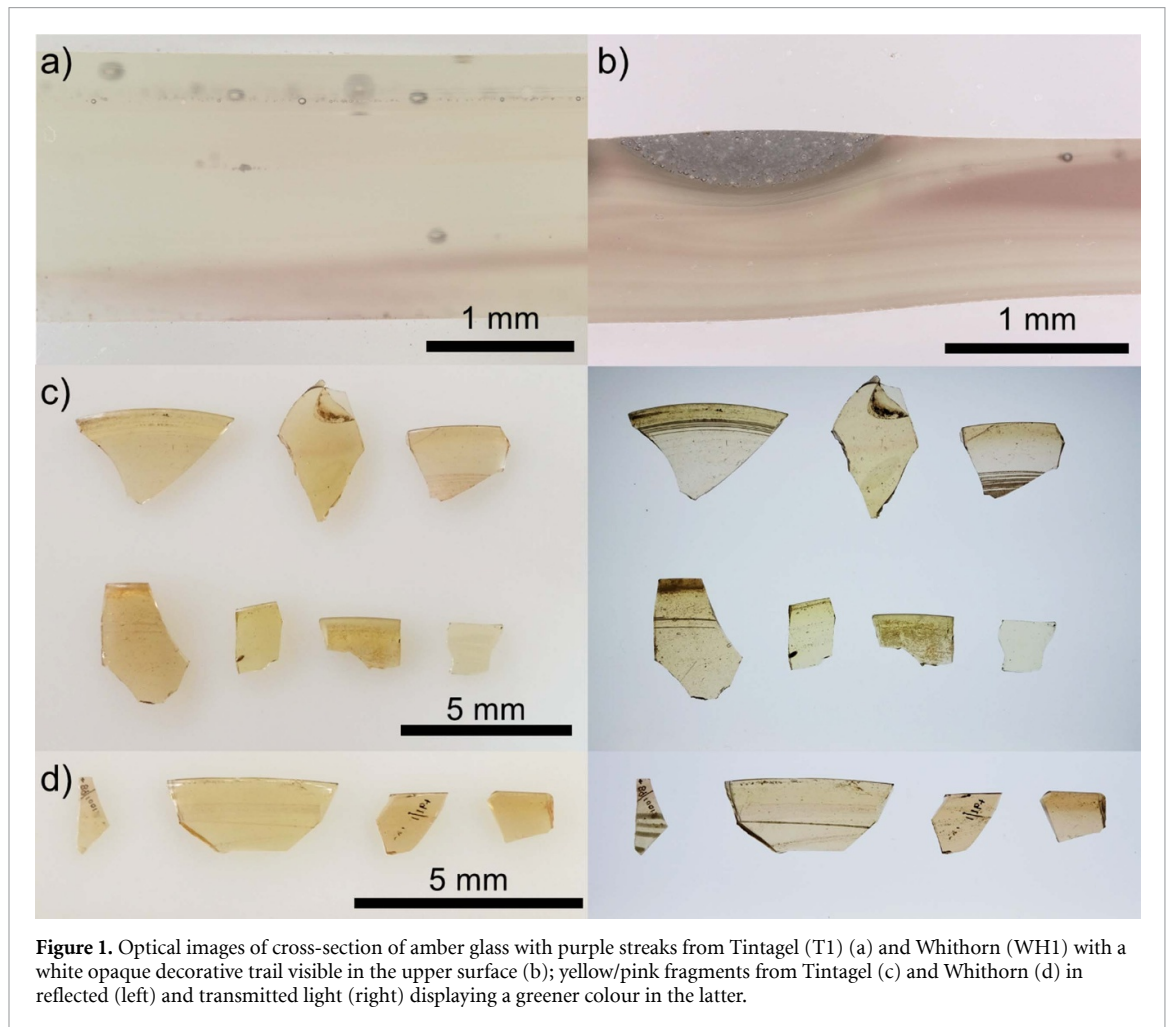
2.2. Methods

2.2.1. 3D digital microscopy

The samples were observed by 3D digital microscopy, using the Keyence VHX7000 3D digital microscope at different magnifications.

Table 1. Summary of the archaeological glass samples from Tintagel and Whithorn. The vessel number refers to the classification in [36].

Sample ID	Small finds number/vessel number	Provenance	Atlantic tradition glass group	Colour
T1	5040	Tintagel	Group D	Yellow with purple streaks
T2	2025	Tintagel	Group B	Light green
T3	3099a	Tintagel	Group C	Yellow
T4	5006	Tintagel	Group B	Green
T5	5096	Tintagel	Group C	Yellow/pink
WH1	16125/Vessel 22	Whithorn	Group C	Yellow with purple streaks
WH2	14429/Vessel 69	Whithorn	Group E	Yellow
WH3	14753/Vessel 67	Whithorn	Group E	Yellow
WH4	1362/Vessel 55	Whithorn	Group D	Yellow

Figure 1. Optical images of cross-section of amber glass with purple streaks from Tintagel (T1) (a) and Whithorn (WH1) with a white opaque decorative trail visible in the upper surface (b); yellow/pink fragments from Tintagel (c) and Whithorn (d) in reflected (left) and transmitted light (right) displaying a greener colour in the latter.

2.2.2. Laboratory bulk XRF spectroscopy
The compositions of the archaeological and experimental glass were determined using a Bruker M4 Tornado bench-top energy dispersive μ-XRF spectrometer. At least three points were analysed for 200 s livetime, with the XRF being operated at 50 kv, 200 μA, in a vacuum with no filter. The results are given in the supporting information (tables S1 and S2).

2.2.3. Scanning electron microscopy combined with an energy dispersive spectrometer (SEM-EDS)
To study the sample morphology and evaluate the presence of nanocrystals or droplets, or weathering layers responsible for the optical properties, the samples were also analysed by SEM combined with an EDS, using a FEI Inspect F, with an Oxford Instruments X-Act SDD and INCA software. The machines (XRF and SEM-EDS) were calibrated using sets of glass standards.

Table 2. Summary of the experimental glass and their characteristics.

Sample ID	Reducing agent (wt%)	MnO_2/Fe_2O_3	Description
S1	0	1.43	Brown glass melted in crucible
S1a	0.10	1.48	Light brown glass melted in crucible
S1b	0.20	1.44	Green glass melted in crucible
S1c	0.15	1.46	Light green glass melted in crucible
S1d	0.13	1.48	Brown glass melted in crucible
S2	0	2.08	Dark brown glass melted in crucible
P1	0	1.45	Dark purple glass melted in pot
P1d	0.13	1.39	Yellow/green glass melted in pot
M1	/	1.40	Yellow/green mixed glass melted in pot
M2i	/	1.40	Purple mixed glass melted in pot and sampled after mixing and melting
M2ii	/	1.38	Purple/amber mixed glass melted in pot and sampled after 1 h
M2iii	/	1.40	Amber mixed glass melted in pot and sampled after 1 d
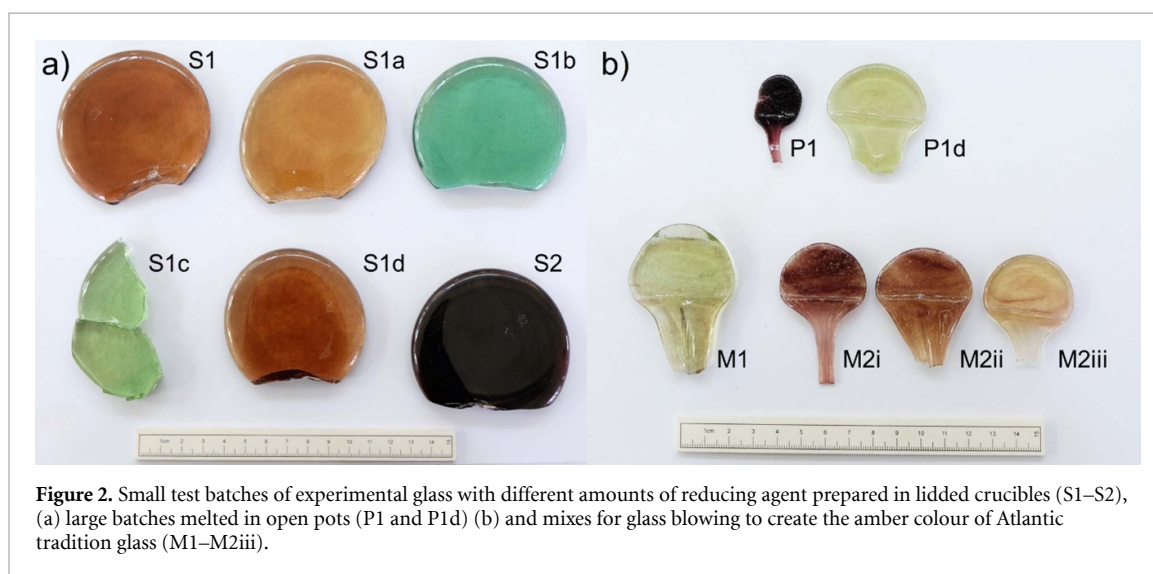
Figure 2. Small test batches of experimental glass with different amounts of reducing agent prepared in lidded crucibles (S1–S2), (a) large batches melted in open pots (P1 and P1d) (b) and mixes for glass blowing to create the amber colour of Atlantic tradition glass (M1–M2iii).

2.2.4. Colorimetry

Colorimetric measurements were performed using a X-Rite Ci62 portable spectrophotometer with a D65 illuminant. Five measurements were carried out on each glass fragment and the data are presented according to the CIE L*a*b* standard colour system.

2.2.5. Synchrotron-based μ-XRF mapping, bulk and μ-XANES spectroscopy at Fe and Mn K-edge

2.2.5.1. Acquisition of bulk XANES data

Fe and Mn speciation measurements of the experimental natron-type glass and the archaeological glass were performed at beamline ID21 of the European Synchrotron Radiation Facility (Grenoble, France) [37]. The energy of the X-ray beam was defined using a Si(111) double crystal monochromator, and scanned from 6.53 to 6.68 keV, with steps of 0.4 eV, for the Mn-edge and from 7.1 to 7.25 keV, with steps of 0.4 eV, for the Fe-edge. The monochromator was calibrated using the first inflection point of the manganese and iron foils (maximum of the first derivative at 6.5515 keV and 7.1271 keV respectively). Macro-XANES spectra were collected using an unfocused beam (300 μm square), in transmission mode for the reference powders, and in XRF mode for the glass samples. For homogenous samples, five points were analysed, and the spectra were normalised and averaged to enhance the signal-over-noise ratio.

The samples were mounted vertically, at an angle of 62° with respect to the incident beam. XRF was collected using a single energy-dispersive silicon drift detector (SGX, 80 mm^2) at 28° of the sample surface.

In addition to the glass samples, reference mineralogical compounds containing iron and manganese in different oxidation states and local geometry were analysed by bulk Fe and Mn K-edge XANES spectroscopy. The minerals containing Fe^{2+} and Fe^{3+} used as references are: almandine ($Fe_3Al_2(SiO_4)_3$ with Fe^{2+}), olivine (($Mg, Fe)_2SiO_4$ with Fe^{2+}), hematite (Fe_2O_3 with Fe^{3+}) and magnetite (Fe_3O_4 with one Fe^{2+} and two Fe^{3+}), following references considered in similar cases [23, 24, 26].

The minerals containing Mn^{2+}, Mn^{3+} and Mn^{4+} used as references are: rhodochrosite ($MnCO_3$ with Mn^{2+}), manganite ($MnO(OH)$ with Mn^{3+}), and pyrolusite (MnO_2 with Mn^{4+}). These reference minerals were finely ground and spread as fine layer on a tape.

The glass samples were analysed embedded in resin in cross-sections.

2.2.5.2. Evaluation of artefacts in XANES data

Before starting the systematic analysis of the samples, preliminary tests were carried out on one of the experimental glasses in order to assess radiation damage caused by the beam to the sample. Experimental conditions were optimized to reduce the dose on the samples: XANES spectra acquired in continuous mode; individual spectra acquired on many different points, rather than cumulating many spectra on the same points, ending in an acquisition time of only $\sim$1 min per spectrum; use of a fast shutter to expose samples to beam only during data collection (in particular closed at the end of each spectrum, when the X-ray energy is sent back to initial value); detector as close as possible to the sample. Once these conditions were set, radiation damage was assessed on two experimental glasses, by consecutively acquiring five XANES spectra on the same point (figure S1). At Fe K-edge, the second spectrum only slightly differs from the first spectrum (shift of the edge towards lower energies; no clear modification of the pre-edge intensity and position), but the next four spectra are similar. At Mn K-edge, no difference is observed among the five consecutive spectra. Based on this result, and despite radiation damage is very low, it was decided to acquire XANES spectra first at Fe K-edge, then at Mn K-edge.

A second possible artefact in this experiment is due to the fact that the XANES spectra were measured in XRF. In this configuration, spectra can be easily distorted by the self-absorption effect depending on the concentration of Fe and Mn. The importance of self-absorption effect was assessed by comparing raw spectra and spectra corrected using the Athena software [38]. Taking into account the matrix composition, no significant changes in the spectra were observed in the range of Fe and Mn concentrations considered here ($\sim$<1%), indicating that self-absorption is here sufficiently low to be neglected (figure S2).

2.2.5.3. Data processing and analysis of XANES data

Analysis of XANES data was done in different ways. After normalization using the PyMca software, spectra were compared and the variation in intensity at two specific energies (7.136 keV for Fe and 6.562 keV for Mn) has been used to qualitatively evaluate the change of Fe and Mn speciation in the different glasses. These energies were selected by considering the highest values of the standard deviation of the spectra collected from the glass samples and are indicated below by a vertical dashed line in figures 3 and 4.

In a second step, XANES spectra were compared using principal component analysis (PCA) with a workflow using the Orange software [39]. PCA was applied on the second derivative of the XANES spectra. PCA scatter plots allow comparing tens of spectra from glasses and references and identifying clusters of spectra. Averages were then calculated over these clusters.
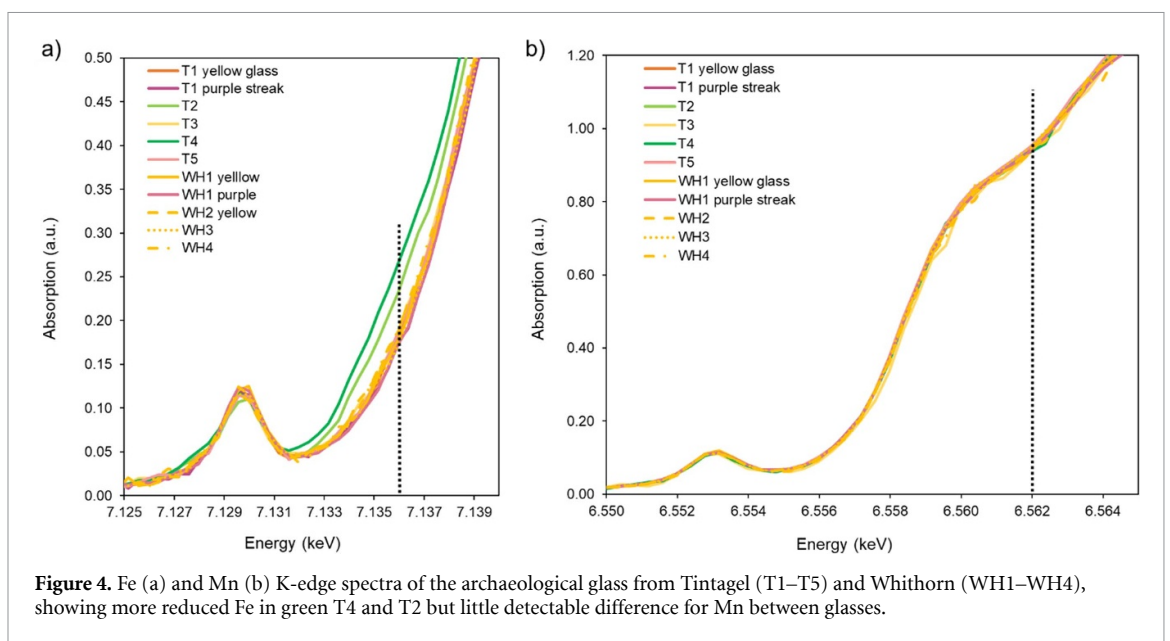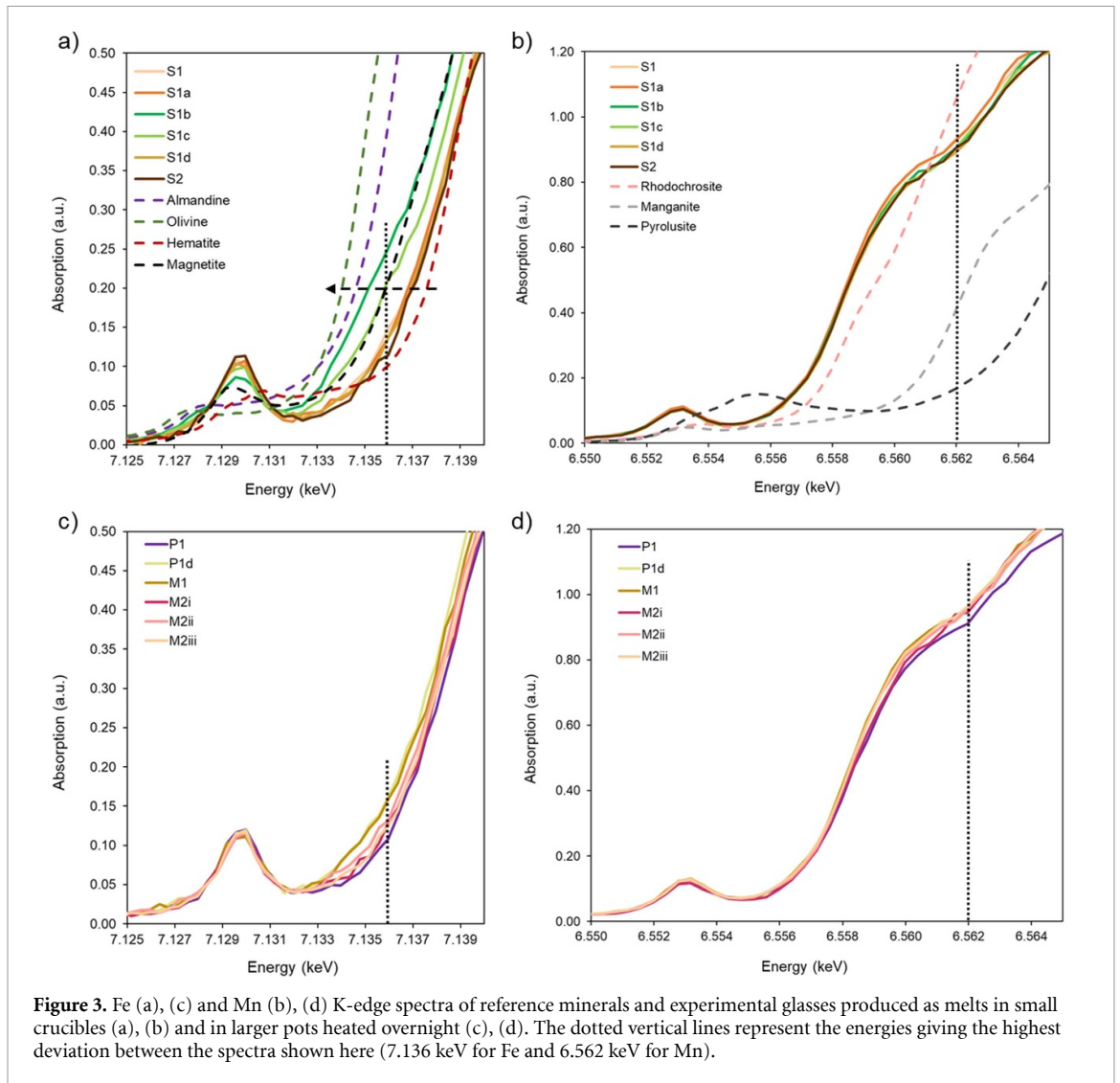
Finally, the analysis focussed on the pre-edge feature of the Fe K-edge XANES spectra, which is particularly sensitive to the valence state and local geometry. The weighted peak position (centroid) shifts to higher energies for increasing ferric to ferrous ratio [30]. The pre-edge peaks of the averaged spectra were fitted with two Gaussians functions as described in the literature using the Larch software [40, 41].

2.2.5.4. Data acquisition, processing and analysis of μ-XRF maps and μ-XANES spectra

The glass samples were also mapped at 7.2 keV by μ-XRF to study the distribution of Fe and Mn in the samples, especially in the archaeological fragments with purple streaks. For these detailed analyses, the beam was focused to 0.23 μm $\times$ 0.80 μm ($v \times h$) using a Kirkpatrick Baez mirror system. The PyMca software was used to fit the μXRF maps, to separate the contribution of different elements, and normalise them with incident intensity [42].

To study the dichroic character of the samples, from the μ-XRF maps, points of interest were selected for the acquisition of μ-XANES spectra of the surface of the glass. In particular several points (every 1 μm) were investigated within the first 20 μm from the surface to compare the oxidation state of Fe and Mn on the surface and in bulk.

Finally, in order to qualitatively map the evolution of Mn speciation from the glass surface to the bulk, the same μXRF map was acquired at a few specific energies in the pre-edge and edge region (from 6.55 to 6.61 keV) and different regions of interest were selected. In the maps presented here, the following energy ranges were selected: E1 from 6.566 to 6.573 keV and E2 from 6.556 to 6.563 keV. The integration of the intensity over these energy ranges was calculated and used to produce the maps.

Figure 3. Fe (a), (c) and Mn (b), (d) K-edge spectra of reference minerals and experimental glasses produced as melts in small crucibles (a), (b) and in larger pots heated overnight (c), (d). The dotted vertical lines represent the energies giving the highest deviation between the spectra shown here (7.136 keV for Fe and 6.562 keV for Mn).

Figure 4. Fe (a) and Mn (b) K-edge spectra of the archaeological glass from Tintagel (T1–T5) and Whithorn (WH1–WH4), showing more reduced Fe in green T4 and T2 but little detectable difference for Mn between glasses.

3. Results

3.1. Influence of different glass production parameters on the experimental glass samples

The experimental glass samples were prepared following the chemical composition of the archaeological glass from Tintagel and Whithorn (tables S1 and S2).

Fe and Mn K-edge XANES spectra acquired from the experimental and archaeological glass fragments show some features that can be linked to the bond distance, oxidation state and site symmetry of these ions. The full spectra are shown in figures S3 and S5, while the close-up of the pre-edge region is displayed in figures 3 and 4.

The comparison of XANES spectra from glasses and from references show that most iron is present as Fe^{3+} and most manganese as Mn^{2+}. The most significant differences in the spectra occurred in the pre-edge region and just above for Fe, and in the main shoulder in the Mn edge.

The Fe K-edge XANES spectra of the small experimental glass batches produced in lidded crucibles (S1–S2) and the reference minerals indicate that by increasing the amount of reducing agent ($KC_4H_5O_6$) in the melt, higher amounts of reduced iron (Fe^{2+}) are produced (especially in samples S1b and S1c) compared to the samples without reducing agent (S1 and S2) (mostly visible in the shift of the edge to lower energies, but also in the presence of a small peak at 7.128 keV in the pre-edge) (figure 3(a)).

From the Mn K-edge spectra of the glass (S1–S2), the addition of the reducing agent in the mix does not lead to a significant modification of XANES spectra (figure 3(b)).

By comparing the results obtained from the small glass batches S1 and S1d and the corresponding larger glass batches made in an open pot (P1 and P1d, respectively), some differences in the spectra can be observed however (figure S4). Iron and manganese are in similar oxidation states in P1 and S1 (large overnight and small test batches respectively), while higher amounts of Fe^{2+} and Mn^{2+} concentrate in large overnight batch P1d compared to small test batch S1d (figure S4). Measuring errors, particularly in the amount of reducing agent added, are more likely to have a significant impact on glass colour and ion speciation in the small batches so the results for the larger batches (M and P series) are considered more reliable. There will be other differences caused by the longer melting duration and larger open pots used for the M and P batches. This highlights the important roles that the geometry and size of the melt container and melting duration play in the modification of the glass redox [25].

Fe-XANES spectra of the batches produced in large open pots without and with reducing agent (P1 and P1d respectively), mixed in different proportion and remelted (M1), and heated for different durations (M2i, M2ii and M2iii) are shown in figure 3(c). They are similar with iron predominantly present in its oxidised (Fe^{3+}) form. P1d and M1 show a slight shift of spectra to lower energies, while M2i–M2iii spectra are intermediate between P1 and P1d-M1.

Regarding Mn, all the glass samples mainly contain manganese in its reduced form (Mn^{2+}), but the glass prepared with a reducing agent (P1d) and the ones obtained by mixing (M) are shifted to lower energies compared to the purple-coloured P1, indicating a higher Mn^{3+}/Mn^{2+} ratio in P1 (figure 3(d)). In addition, remelting and reheating the mixed batches (M2i) for 1 h (M2ii) and 24 h (M2iii) results in less Mn^{3+} in the glass, as the longer melting duration promotes the conversion of Mn ions (in excess compared to Fe) into Mn^{2+}.

3.2. Fe and Mn concentration and speciation in the archaeological glass from Tintagel and Whithorn

The average of Fe and Mn K-edge XANES spectra collected from the archaeological glass fragments from Tintagel (T1–T5) and Whithorn (WH1–WH4) are shown in figures 4 and S5. They are very similar, indicating that iron and manganese are present in a similar oxidation state in all the yellow samples, with mainly Fe^{3+} and Mn^{2+}. The Fe pre-edge and edge position shows that the green glass samples (T2 and T4) are slightly more reduced than T1, T3, T5 and WH1–WH4 (figure 4(a)).

In the yellow samples with purple streaks (T1 and WH1), different XANES spectra were collected in the yellow and purple areas to assess any changes in Fe and Mn oxidation states. No detectable differences could be observed in neither Fe nor Mn XANES spectra between these areas in the same sample (figure 4).

However, considering the limitations of XANES with glass samples discussed above, the presence of a small and subordinate amount of Mn^{3+}, which would be responsible for the purple colour of the streaks, could not be discounted [23, 28]. Previous studies indicate that even a small amount of Mn^{3+} can produce purple to light pink colours [43]. In particular, an Mn^{3+}/Mn_{total} ratio of about 4% was found in purple glasses and considered to be the main agent influencing the colour saturation [28].

The graphs in figure 5 show the intensity of the edge position at 7.136 keV and at 6.562 keV for Fe and Mn, respectively, in the XANES spectra acquired from the experimental and archaeological glass fragments in relation to the Mn/Fe ratio. With intensity values higher than 0.22 at 7.136 keV in the Fe spectra, the glass
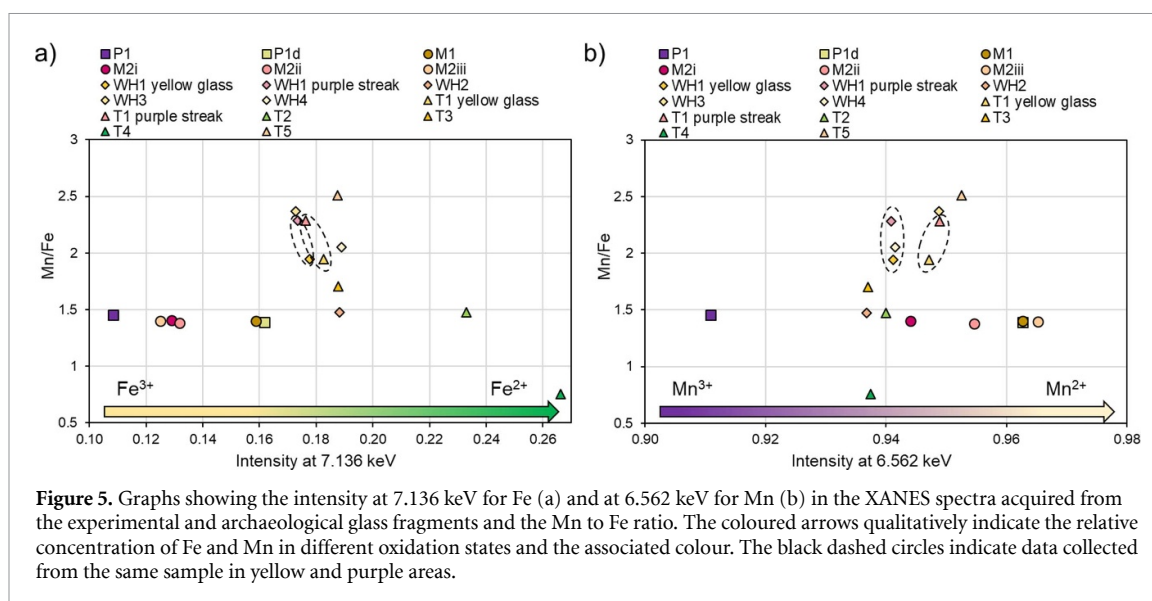
Figure 5. Graphs showing the intensity at 7.136 keV for Fe (a) and at 6.562 keV for Mn (b) in the XANES spectra acquired from the experimental and archaeological glass fragments and the Mn to Fe ratio. The coloured arrows qualitatively indicate the relative concentration of Fe and Mn in different oxidation states and the associated colour. The black dashed circles indicate data collected from the same sample in yellow and purple areas.

appears green (T2) and (T4), as more reduced iron is present (figure 5(a)). With intensity values lower than 0.92 at 6.562 keV in the Mn spectra, the glass is purple (P1) due to higher amount of Mn^{3+} (figure 5(b)).

The intensity at 7.136 keV and at 6.562 keV in Fe and Mn XANES spectra, respectively, is in the same range in both the yellow experimental and yellow archaeological glass, indicating that Fe and Mn are mainly in the same speciation in all the glasses. Compared to P1 (a purple experimental glass) however, Fe and Mn are more reduced in the yellow/amber archaeological samples. As evidenced by the data obtained from M2i, M2ii and M2iii, the Mn^{3+} content in the glass decreases by reheating the same batch of glass, as more manganese gets reduced to reach equilibrium conditions, according to equation (1). The colour of these fragments changes from purple (M2i) to amber with purple streaks (M2iii) after reheating for 24 h.

These data suggest that the yellow ancient glasses were produced by mixing green glass with small amounts of purple glass containing Mn^{3+}. This ensured that the final glass would have a yellow/pink colour instead of green, and also explains the presence of purple streaks in some of the yellow archaeological fragments.

Except for T4, which has a Mn to Fe ratio lower than 1, the ratio of Mn to Fe in the majority of the experimental and archaeological glass is between 1.4 and 1.9 (tables S1 and S2). Some amber-yellow archaeological glasses (T5, WH3 and WH4) display a higher Mn/Fe ratio (from 2 to 2.5) (figure 5). Despite having a higher content of Mn, the majority of manganese is present as Mn^{2+}, and so the colour of the glass is still amber/yellow. The results obtained from the yellow archaeological glass samples with purple streaks (T1 and WH1, highlighted in black dashed circles) indicate that the Mn/Fe ratio is higher in the purple streaks as the glass has not been fully homogenised. Although the majority of the Mn is present in the same oxidation state in the yellow and purple areas, some Mn^{3+} must persist in the purple regions due to the additional Mn and non-equilibrium conditions, causing the difference in colour in these areas.

This result was confirmed also by elemental maps obtained by SR-μXRF (figure 6), showing that manganese concentrates in the purple areas and streaks.

PCA was used to further compare the individual spectra acquired at Fe and Mn K-edges on both the experimental and archaeological samples and better highlight their differences, taking into account the entire white line region, rather than the absorption intensity at a specific energy. The first component for Fe XANES represents only 38% of the variance, showing the high heterogeneity of the dataset. Conversely, PC1 for Mn spectra represents 64% of the variance, and indeed reflects a much lower dispersity of the dataset.

The position of the Fe reference materials in the PCA scatter plot shows oxidized iron (Fe^{3+}) concentrates in low PC1 while references with Fe^{2+} shifts to high PC1.

In the PCA applied to the Fe spectra, three main groups were identified (figure 7(a)):

(1) Group Fe_1 (purple circle): experimental glasses produced in larger pots and heated overnight.
(2) Group Fe_2 (orange circle): yellow/amber archaeological glasses.
(3) Group Fe_3 (green circle): green archaeological glasses.

The average Fe K-edge spectra of the three groups are shown in figure 8 and confirm the shift of the edge to lower energies from group Fe_1 to Fe_3, related to the increased Fe^{2+}/Fe^{3+} ratio. The graph further
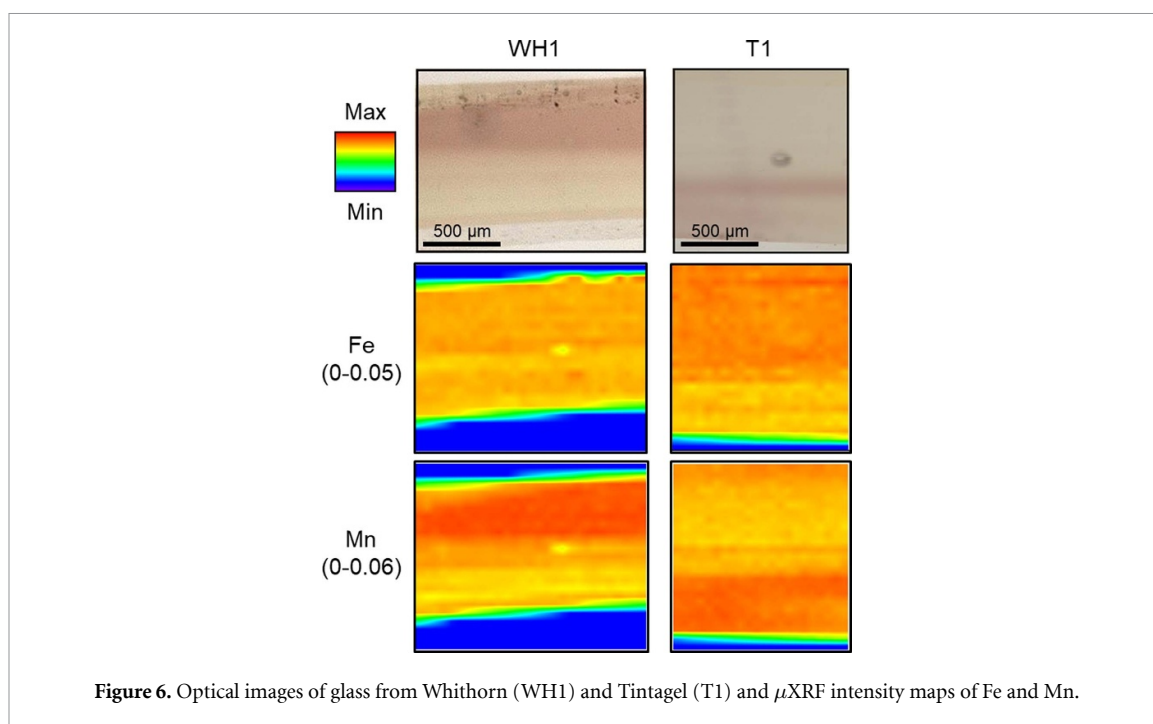
Figure 6. Optical images of glass from Whithorn (WH1) and Tintagel (T1) and μXRF intensity maps of Fe and Mn.

supports the hypothesis that the yellow/amber ancient glasses were produced by mixing, but often not completely homogenising, green glass with additional purple glass.

For Mn XANES spectra, the reference materials distribute from along a diagonal (PC1–PC2) with increasing oxidation states. The points acquired on glasses could not provide clear clustering, confirming the difficulties in detecting modification of the Mn valence state in glasses (figure 7(b)). Despite this, it can be noted that the samples which have theoretically a higher Mn^{3+}/Mn^{2+} ratio seem to place at higher PC1 than the other in the plot.

Two average spectra were however calculated on two groups of samples (group Mn_1: experimental glass samples; and group Mn_2: archaeological glass).

To further identify the Fe speciation in the three different clusters, the pre-edge peaks of the averaged spectra of each group have been fitted using two Gaussian functions that can be linked to the oxidation state of Fe [40] (figure 8). From these fits, it is very clear that the area of the peak at lower energy, which can be associated to Fe (II), increases from group Fe_1 to group Fe_3. This is also visible in the centroid position of the peaks, which shifts from 7129.32 eV for group Fe_1 to 7129.52 for group Fe_2 and 7129.54 for group Fe_3 (the calculated errors for the centroids positions are of 0.04 eV). It should be noted here that the energy positions are higher than the ones usually found in the literature due to the monochromator calibration (see materials and methods part 2.2.5).

Pre-edge peak fitting of the group Mn_1 (experimental glass samples) and Mn_2 (archaeological glass samples) average spectra did not reveal any trend, further highlighting the previously mentioned difficulties regarding this element (figure S6).

3.3. Correlation of Fe and Mn content and speciation and glass colours

Colorimetric measurements were collected from the experimental and archaeological glass fragments, aiming to correlate the colour with the Fe and Mn content and oxidation states (table S3). The coordinates a* (red-green hues) and b* (blue-yellow hues) indicate the colour of these samples.
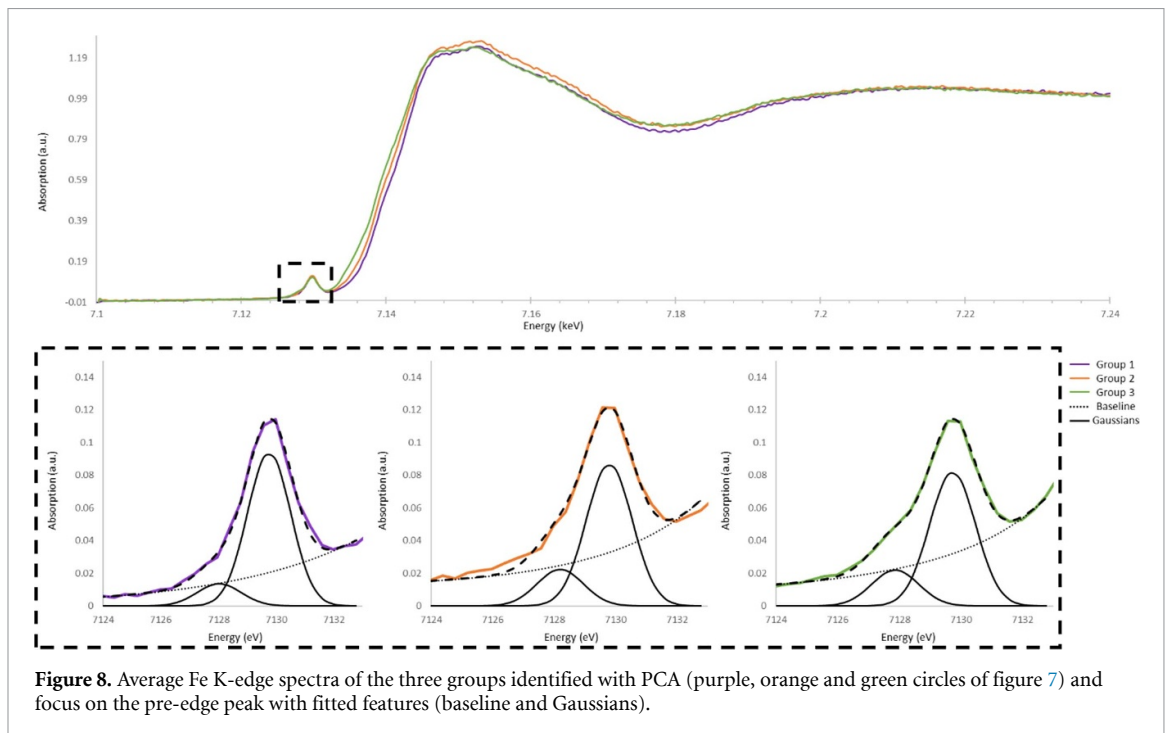
As shown in figure 9(b), the amount of reduced iron in the glass is correlated with a*, because green glass contains more Fe^{2+}, as evidenced by the small test samples produced with the reducing agent (S1b and S1c) and archaeological glasses T2 and T4. The content of ferrous iron is lowest in purple and brown (P1, S1, S1d, S2 and M2i) and amber-coloured glasses (S1, M1, M2ii and M2iii).

Conversely, figure 9(b) shows that purple and dark brown fragments (P1 and S2) have the lowest b* values and they contain the lowest Mn^{2+} content.

The yellow glasses display intermediate features. The majority of them still contain some reduced iron and manganese is mostly in its reduced form. However, in some of them manganese is also present as Mn^{3+} (T3, WH1, WH2 and WH4). This corroborates the theory that these yellow glass samples are the result of
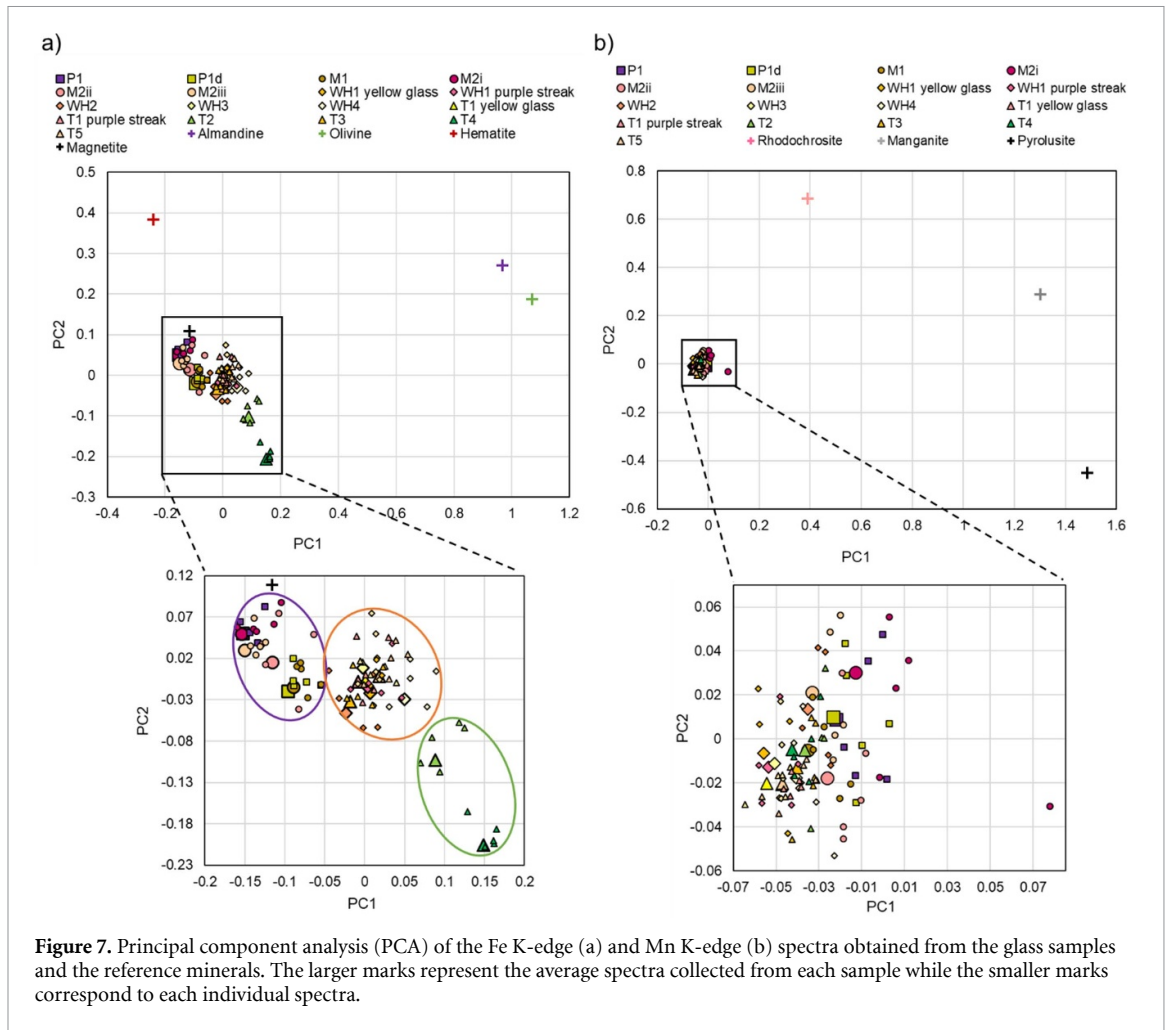
Figure 7. Principal component analysis (PCA) of the Fe K-edge (a) and Mn K-edge (b) spectra obtained from the glass samples and the reference minerals. The larger marks represent the average spectra collected from each sample while the smaller marks correspond to each individual spectra.

Figure 8. Average Fe K-edge spectra of the three groups identified with PCA (purple, orange and green circles of figure 7) and focus on the pre-edge peak with fitted features (baseline and Gaussians).

Figure 9. Graphs plotting the chromatic coordinates a* and b* of the experimental (S1-M2iii) and archaeological (T1-WH4) glass fragments showing the influence of Fe^{2+} (a) and Mn^{2+} (b). In the graph on the left (a), the size of the markers (small, medium and large) represents the three groups identified with PCA (Fe_1, Fe_2 and Fe_3, respectively), which are related to increased Fe^{2+}/Fe^{3+} ratio. In the graph on the right (b), the size of the markers (small and large) is related to the experimental (Mn_1) and archaeological (Mn_2) glass samples, respectively. The arrows indicate the colour shifts in samples M2i, M2ii and M2iii.

mixing green/yellow glass with small amounts of purple glass. In particular, the purple streaks in some yellow glasses are produced due to incomplete mixing of the purple glass.

As previously pointed out, by reheating the same glass batch for 1 and 24 h (M2i-M2iii) the Mn^{2+} content increases, resulting in a colour shift from purple to amber with purple streaks (figure 9(b)).

### 3.4. Study of the optical characteristics of some archaeological samples

Some of the archaeological glass samples belonging to the Atlantic tradition look pink/yellow when observed in reflected light but light green in transmitted light (figure 1). Dichroism is sometimes observed in archaeological glass, and is usually caused by the presence of metal nanoparticles or the separation of colloidal droplets that scatter light. Neither small crystals nor droplets were found in the fragments from Tintagel and Whithorn observed by SEM-EDS (figure S7). One hypothesis for the appearance of these fragments is the presence of thin weathered layers with different optical properties on the glass surface. Similar to modern dichroic filters for glass used in design and architecture, which are composed of nanometric layers with different features, the presence of surface layers on the archaeological glass can selectively transmit or reflect some light wavelengths, resulting in different colour and visual effects according to the lighting conditions.

To investigate this hypothesis, surface areas of the archaeological samples displaying these optical characteristics were analysed by SR-μXRF and Fe and Mn K-edge XANES with a focused beam and compared with the experimental sample M2i, which has no surface weathering.

SEM BSE imaging shows the presence of a weathered surface layer on most of the samples (figure S7). The weathered layers are variable in thickness and integrity, influenced not only by the glass composition, but also by the burial and post-burial environments, excavation technique (by hand from environmental samples), cleaning, handling and storage since recovery. In general, the weathering layer is more pronounced in the fragments with a higher ratio of alkali modifiers to network stabilisers, which influences glass stability, but is rarely more than 10 μm thick overall. Some weathering layers show cracks, pores and poor integrity in the SEM images (figures S7 and S8).

This variability is reflected in the SR-μXRF results, as two broad types of surface layer were identified: the first one comprises fragments (T1, WH3 and M2i) with the uppermost layer enriched in silicon, followed by a layer with some indication of enrichment in manganese; the samples belonging to the second group (T3, T5 and WH1) exhibit a thin top layer rich in iron (figure 10). In the first case, the presence of the silicon-rich layer can be due to post-burial weathering [44–46] or, as in the case of the experimental glass, due to leaching of particles from the melt container or incomplete glass mixing. The increased concentration of iron at the surface of some samples may be due to iron contamination from the soil post burial.

To evaluate any changes in the speciation of Fe and Mn ions on the glass surface and in the bulk, Fe and Mn K-edge μXANES spectra were collected every 1 μm from the surface of the archaeological and experimental samples (within 20 μm) (figures 11 and S9). The archaeological samples show a trend: the intensity of the edge position at 6.562 keV (in Mn spectra) increases from the surface to the bulk (20 μm). An increase in intensity indicates a higher concentration of Mn^{2+} species, so the trend highlights that a
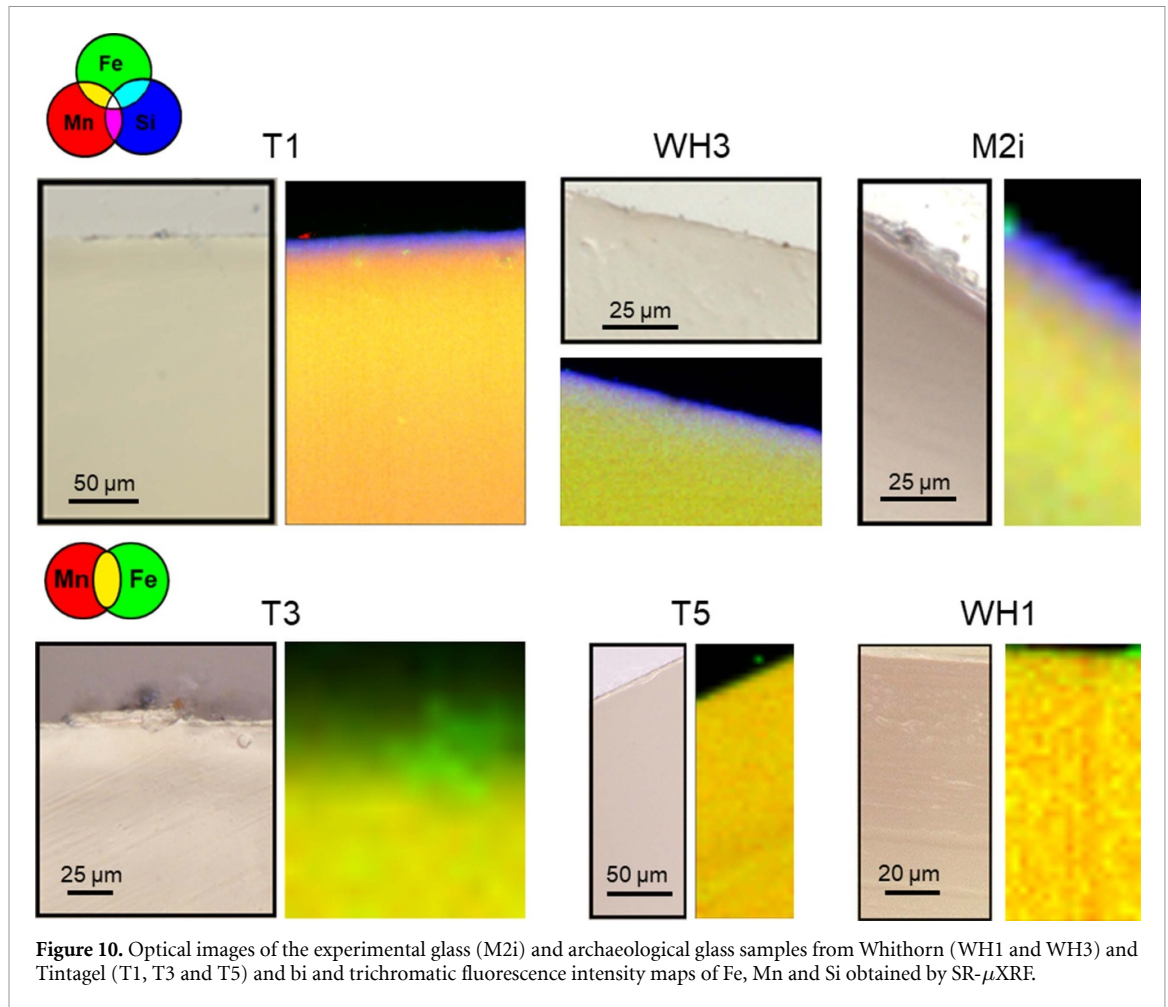
Figure 10. Optical images of the experimental glass (M2i) and archaeological glass samples from Whithorn (WH1 and WH3) and Tintagel (T1, T3 and T5) and bi and trichromatic fluorescence intensity maps of Fe, Mn and Si obtained by SR-μXRF.
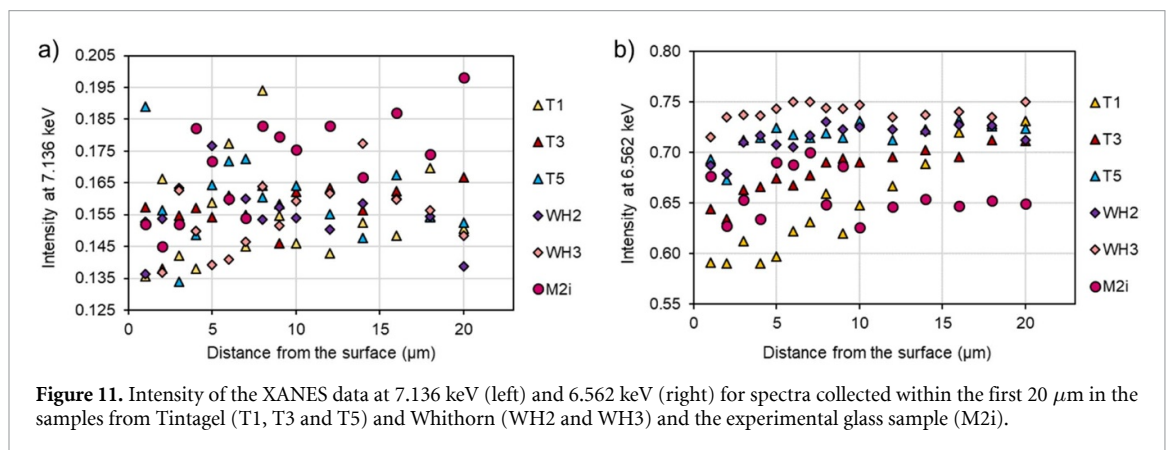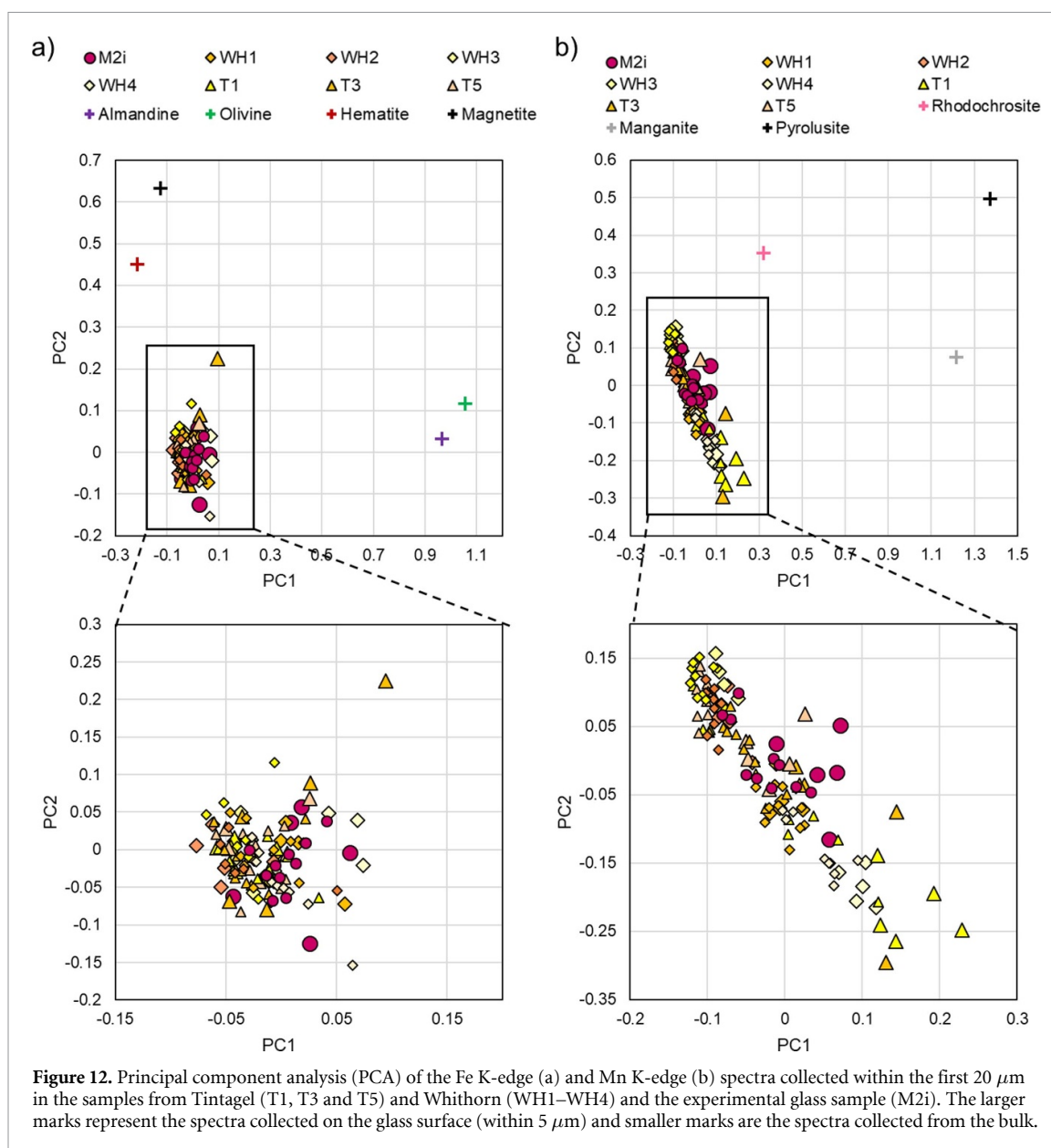

Figure 11. Intensity of the XANES data at 7.136 keV (left) and 6.562 keV (right) for spectra collected within the first 20 μm in the samples from Tintagel (T1, T3 and T5) and Whithorn (WH2 and WH3) and the experimental glass sample (M2i).

higher amount of reduced manganese is present in the bulk (figure 11(b)). The oxidation state of manganese in M2i does not follow this trend. The increase in Mn oxidation state is seen mainly within 10 μm of the glass surface, which corresponds to the approximate thickness of weathering layer seen on the archaeological samples (figure S7(g)).

The speciation of iron in the archaeological and experimental glass varies from the surface to the bulk, but it does not follow a pattern as manganese (figure 11(a)), most probably because it is mainly present as Fe^{3+} throughout the glass.

PCA was used to further highlight the differences in the individual spectra acquired at Fe and Mn K-edges on both the experimental and archaeological samples (figure 12). The first component calculated for Fe XANES only explains 24% of the cumulated variance, which is low for a first component, and illustrates that there is no strong tendency and a high heterogeneity in this dataset. In addition, this component does not display any correlation with the depth at which the spectra were recorded, further confirming the lack of

Figure 12. Principal component analysis (PCA) of the Fe K-edge (a) and Mn K-edge (b) spectra collected within the first 20 μm in the samples from Tintagel (T1, T3 and T5) and Whithorn (WH1–WH4) and the experimental glass sample (M2i). The larger marks represent the spectra collected on the glass surface (within 5 μm) and smaller marks are the spectra collected from the bulk.
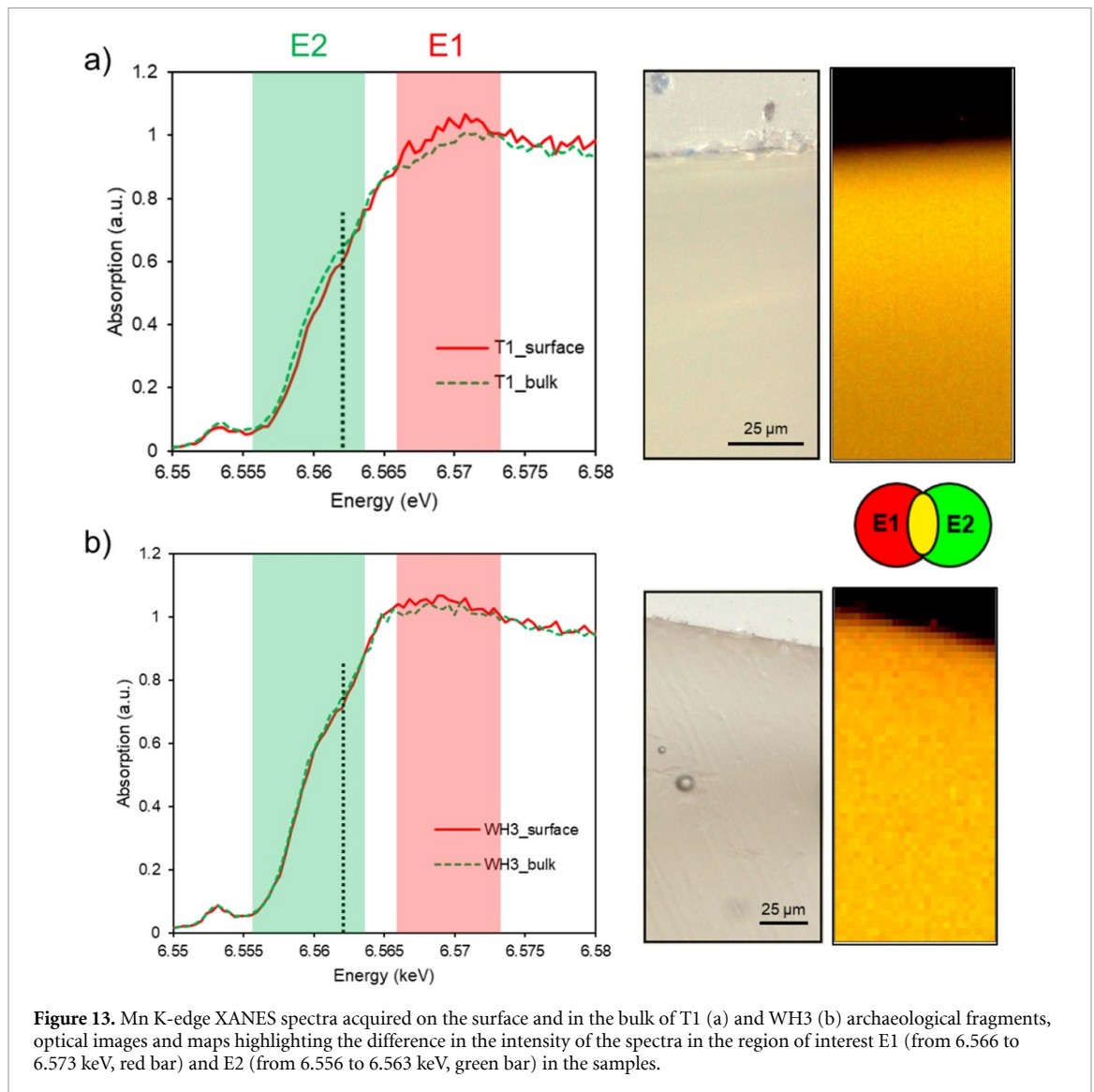
trend. Conversely, PC1 for Mn spectra already explains 47% and PC2 still explains 19% of the cumulated variance. It can also be observed that Mn spectra collected on the surface of the glass (shown as bigger points in figure 12, with one different colour per sample) are concentrated at higher PC1 and lower PC2. This suggests that the two PCs are indeed correlated to a depth-related change in the spectra linked to the Mn oxidation state.

To evaluate the distribution of Mn in different oxidation states along the archaeological glass samples, speciation maps were obtained (figure 13). These samples (T1 and WH3) contain the highest levels of manganese amongst the glass studied (together with WH1 and T5). Both Mn-XANES spectra and the speciation maps indicate a shift of the edge to higher energies, from bulk to surface. This is correlated with higher concentration of oxidised manganese in the surface than in the bulk of the samples. Indeed, the intensity of the spectra in the region of interest E2 (from 6.554 to 6.595 keV), which is correlated with higher concentration of reduced manganese, is lower on the surface than in the bulk of the samples.

This surface layer where Mn is more oxidised in some of the archaeological fragments is believed to scatter transmitted and reflected light differently and to be responsible for the pinker hue of the glass in reflected light. This result is consistent with the observation in some of the glasses of a more purple surface layer than the underlying yellow glass (figure S8).

The fact that Mn in the experimental glass M2i is not more oxidised than the bulk suggests that the formation of the surface layer in the archaeological samples occurs post-burial, and is localised to the 10 μm surface region where there is weathering and alteration of the glass, rather than during manufacture. A

Figure 13. Mn K-edge XANES spectra acquired on the surface and in the bulk of T1 (a) and WH3 (b) archaeological fragments, optical images and maps highlighting the difference in the intensity of the spectra in the region of interest E1 (from 6.566 to 6.573 keV, red bar) and E2 (from 6.556 to 6.563 keV, green bar) in the samples.

weathering layer with similar properties may be present in other examples of contemporary archaeological glass with high concentrations of manganese, but it has been noticed in the case of the Atlantic tradition glass because the glass bulk has a very pale colour, against which the pinker surface discolouration is more apparent.

4. Discussion

The Atlantic tradition glass displays unique features (colour and quality), which distinguish it from contemporary glass with the same composition from Anglo-Saxon sites in Britain and France, emphasising the presence of different material cultures in Britain at this time.

This study of experimental and archaeological glass fragments evaluated the impact of different parameters (such as the chemical composition, the iron and manganese speciation, the glass heterogeneity, and the optical character of the surface) on the appearance of the glass, to unravel the colouring techniques used by the glassworkers.

As highlighted in other studies [25, 28], the amount of manganese in proportion to iron significantly affects the glass colour.

Iron and manganese speciation also has an impact on the glass colour, as higher concentrations of iron in its reduced form are necessary to make the glass green or blue. This was proved in the green experimental glasses (S1b and S1c) produced by adding a reducing agent to the melt. In the past, carbon sources were used for this purpose [25] and they were able to reduce both iron and manganese (see experimental sample P1d).

With higher Mn/Fe ratios, the glass colour ranges from purple to yellow/amber, depending on the oxidation states of iron and manganese. Purple glasses (P1 and M2i) are more oxidised as they contain higher

amounts of oxidised manganese compared to yellow glasses. Even small fractions of Mn^{3+}, which are difficult to detect using XANES, are able to shift the colour to purple. Despite Mn^{3+} and Mn^{4+} being unstable at the temperatures used in glass production, it is likely that purple glasses were obtained in unusual oxidising conditions, with a short melting duration and careful selection of the raw materials, which may have been subjected to thermal treatments [25, 28]. The difficult and unusual production conditions necessary to obtain purple glass, and retain the colour through subsequent reheating and recycling, would explain the scarcity of the colour [28].

Some yellow/amber archaeological fragments contain higher Mn/Fe ratios than the experimental purple glass made for this study (P1 and M2i), because Mn is mainly present in its reduced form. The results obtained from the study of amber fragments with purple streaks indicate that the majority of the manganese is in the same speciation (mainly Mn^{2+}) in the yellow and purple areas, but that there is a higher concentration of manganese in the streaks and it is likely that there is a small proportion of strongly colouring Mn^{3+} ions remaining in those areas as well, although these are difficult to detect with XANES, as already observed by Capobianco *et al* [28].

The Atlantic West glass was therefore probably made by remelting green glass (green being richer in Fe^{2+} than yellow glass) with some purple fragments (richer in Mn^{3+}). This would explain the remnants of purple streaks in some of the amber archaeological glass, which remain due to incomplete mixing of the melt.

In the experimental glasses, the size of the batch (and resulting weighing errors), the shape and size of the melt container (and whether lidded or not) and the melting conditions and duration influenced the glass heterogeneity and colour, without changing the chemical composition. In particular, by extending the melting duration from 1 to 24 h, the melts became more homogenous and more manganese reduces, resulting in a colour shift from purple to amber (see samples M2i, M2ii and M2iii). This finding is not in agreement with the study by Bidegaray *et al* [25] recreating Roman purple glass, in which no significant differences in manganese and iron speciations were found for melting times of 7 and 32 h. The Bidegaray experiments used small batches of 100 g, which were fully homogenised by repeatedly cooling, crushing and re-melting the glass whereas the glass batches M2i to M2iii in this study were much larger and composed of a mixture of green and purple glass (albeit with the same chemical composition). This result further emphasises a key feature of the late Antique archaeological glass, which is its heterogeneity in terms of manganese concentration and speciation, and this supports the conclusion that green and a small amount of purple glass were recycled together to obtain the Atlantic West tradition amber glass. Bidegaray concluded that the control of colour in manganese-containing glass was dominated by the action of oxidising or reducing additives added to the melt rather than external factors, such as exchange of oxygen with the furnace atmosphere; in the case of the Late Antique glass studied here, the addition of a small amount of purple glass to the batch is effectively acting as an oxidising additive. Purple glass was rare and precious, therefore, its addition to the melt is most probably a deliberate choice to obtain this specific colour. As this type of glass was produced over a considerable period, it suggests there was continuing access to supplies of purple glass in the production centres. The shape and colour of these drinking vessels may have a cultural significance in the Atlantic West region of Britain, and might be associated with specific types of drinks.

The unusual optical properties of some of the amber archaeological fragments were also investigated. Neither nanoparticles nor small droplets, which can cause dichroism, were found in the samples. Some samples display a detectable surface layer richer in silicon and manganese, while increased iron is detected in others, potentially due to contamination post-burial. XANES spectra and speciation maps suggest that manganese is more oxidised in the most superficial layers of the glass than the bulk, while iron speciation is not affected. The presence of a surface layer richer in Mn^{3+} might be responsible for scattering transmitted and reflected light differently, imparting seemingly dichroic properties to the glass. This surface layer is present only in the archaeological samples and not in the experimental ones, indicating a probable formation post-burial (possibly related to soil pH), rather than during their production. Although the precise cause of this effect is unknown, changes in manganese oxidation state have been observed in historical and archaeological glasses previously, for example due to solarisation. Several researchers have reported the impact of the exposure for extended periods of time to UV-light irradiation on the photo-oxidation of Mn^{2+} to Mn^{3+} in colourless glass, producing purple areas [34, 47–49]. Here, a surface layer with more oxidised Mn absorbs and transmits different light wavelengths than the glass underneath, resulting in colour changes.

5. Conclusions

The opportunity to apply synchrotron techniques to study archaeological glass from Tintagel and Whithorn (UK) allowed a thorough investigation of the colouring technologies used by glassmakers in the 5th–7th centuries to make the unusual glass so characteristic of the Atlantic West of Britain. This type of glass is pale

yellowish to amber coloured, sometimes with purple streaks, and it is distinctly different from the glass found further east in Anglo-Saxon England, which is usually darker green or brown.

The impact of different production parameters (chemical composition, reducing/oxidising conditions, recycling) was investigated by preparing experimental glass samples.

Fe and Mn XANES spectra of the archaeological glass samples indicate that Fe and Mn are in similar oxidation states in all of the yellow samples (3+ and 2+ respectively), while iron is more reduced in the green samples.

No detectable difference in Mn and Fe oxidation state occurs in the purple stripes compared to the yellow glass bulk, suggesting that only a small (and therefore not detectable) proportion of the Mn ions are present as 3+ but that these are strongly colouring. μXRF maps of the distribution of Fe and Mn in the samples demonstrated that higher concentrations of Mn are present in the purple streaks in the samples. Accordingly, in this case, it is concluded that the colour of these regions is due to a combination of increased Mn/Fe ratio with a proportion of those Mn ions present as strongly coloured 3+. This suggests that the Atlantic tradition glass was produced by mixing green glass with some purple and that the remains of purple streaks in some archaeological samples are due to incomplete mixing, in an effort to retain the distinctive colour.

Many archaeological fragments display distinctive optical effects, as they appear pale green in transmitted light but pinkish to amber-coloured in reflected light. Results obtained by μXANES spectra and maps suggest the post-burial formation of a surface layer, where Mn is more oxidised and therefore purple, which is believed to scatter transmitted and reflected light differently. When viewed against the pale colour of the glass bulk, this layer is likely to be responsible for these apparent colour changes. The preparation of mock-up samples subjected to accelerated ageing to simulate the burial environment could enable the assessment of this hypothesis.

Data availability statement

The data that support the findings of this study are available upon reasonable request from the authors.

Acknowledgments

ORCID iD

Francesca Gherardi ⬤ https://orcid.org/0000-0003-0469-8154

References

[1] Evison V I 2000 Glass VESSELS in England AD 400–1100 *Glass in Britain and Ireland AD 350–1100* vol 127, ed J Price (British Museum Occasional Paper) pp 47–104

[2] Evison V I 2008 *Catalogue of Anglo-Saxon Glass in the British Museum* (British Museum)

[3] Freestone I C and Gorin-Rosen Y 1999 The great glass slab at Bet She'arim, Israel: an early Islamic glassmaking experiment? *J. Glass Stud.* **41** 105–16

[4] Galili E, Gorin-Rosen Y and Rosen B 2015 Mediterranean coasts, cargoes of raw glass *Hadashot Arkheologiyot, Excavations and Surveys in Israel* vol 127 (Israel Antiquities Authority)

[5] Nenna M D 2015 Primary glass workshops in Graeco-Roman Egypt: preliminary report on the excavations of the site of Beni-Salama, Wadi Natrun (2003, 2005–2009) *Glass of the Roman World* ed J Bayley, I C Freestone and C M Jackson (Oxbow Books) pp 1–22

[6] Freestone I C, Gorin-Rosen Y and Hughes M J 2000 Primary glass from Israel and the production of glass in late antiquity and the early Islamic period *Proc. of the Colloque Organisé En 1989 Par l'Association Française Pour l'Archéologie du Verre (AFAV)*

[7] Jackson C M, Paynter S, Nenna M D and Degryse P 2018 Glassmaking using natron from el-Barnugi (Egypt); Pliny and the Roman glass industry *Archaeol. Anthropol. Sci.* **10** 1179–91

[8] Jackson C M and Paynter S 2016 A great big melting pot: exploring patterns of glass supply, consumption and recycling in Roman Coppergate, York* *Archaeometry* **58** 68–95

[9] Paynter S and Jackson C M 2016 Re-used Roman rubbish: a thousand years of recycling glass *Eur. J. Postclass. Archaeol.* **6** 31–52

[10] Schibille N, Meek A, Tobias B, Entwistle C, Avisseau-Brousset M, Da Mota H and Gratuze B 2016 Comprehensive chemical characterisation of byzantine glass weights *PLoS One* **11** e0168289

[11] Campbell E 2000 A review of glass vessels in Western Britain and Ireland AD 400–800 *Glass in Britain and Ireland AD 350–1100* ed J Price (British Museum Occasional Paper) pp 33–46

[12] Campbell E 2007 Glass *Excavations at Tintagel Castle, Cornwall, 1990–1999* vol 74, ed R C Barrowman, C E Batey and C D Morris (Reports of the Research Committee of the Society of Antiquaries of London, Society of Antiquaries) pp 222–8

[13] Campbell E 2007 Continental and Mediterranean imports to Atlantic Britain and Ireland, AD 400¬-800 *Counc. Br. Archaeol. Res. Rep.* **157**

[14] Campbell E Glass unpublished complete glass report from 20th-century excavations at Tintagel Castle

[15] Velde B 1990 Alumina and calcium oxide content of glass found in Western and Northern Europe, first to ninth centuries *Oxford J. Archaeol.* **9** 105–17

[16] Wedepohl K H, Pirling R and Hartmann G 1997 Römische und fränkische Gläser aus dem Gräberfeld von Krefeld-Gellep *Bonner Jahrbücher* **197** 177–89

[17] Mirti P, Lepora A and Saguì L 2000 Scientific analysis of seventh-century glass fragments from the Crypta Balbi in Rome *Archaeometry* **42** 359–74

[18] Foy D, Picon M, Vichy M and Thirion-Merle M 2003 Caractérisation des verres de la fin de l'Antiquité en Méditerranée occidentale: l'émergence de nouveaux courants commerciaux *Échanges et Commerce du Verre Dans le Monde Antique: Actes du Colloque de l'Association Française Pour L'archéologie du Verre Aix-en-Provence et Marseille* ed D Foy and M D Nenna (Monique Mergoil) pp 41–85

[19] Freestone I C, Hughes M J and Stapleton C P 2008 The composition and production of Anglo-Saxon glass *Catalogue of Anglo-Saxon Glass in the British Museum* ed V I Evison (British Museum) pp 29–46

[20] Foster H E and Jackson C M 2009 The composition of 'naturally coloured' late Roman vessel glass from Britain and the implications for models of glass production and supply *J. Archaeol. Sci.* **36** 189–204

[21] Ceglia A, Cosyns P, Nys K, Terryn H, Thienpont H and Meulebroeck W 2015 Late antique glass distribution and consumption in Cyprus: a chemical study *J. Archaeol. Sci.* **61** 213–22

[22] Cholakova A, Rehren T and Freestone I C 2016 Compositional identification of 6th c. AD glass from the Lower Danube *J. Archaeol. Sci.* **7** 625–32

[23] de Ferri L, Arletti R, Ponterini G and Quartieri S 2011 XANES, UV-VIS and luminescence spectroscopic study of chromophores in ancient HIMT glass *Eur. J. Mineral.* **23** 969–80

[24] Arletti R, Quartieri S and Freestone I C 2013 A XANES study of chromophores in archaeological glass *Appl. Phys.* A **111** 99–108

[25] Bidegaray A-I, Godet S, Bogaerts M, Cosyns P, Nys K, Terryn H and Ceglia A 2019 To be purple or not to be purple? How different production parameters influence colour and redox in manganese containing glass *J. Archaeol. Sci.* **27** 101975

[26] Quartieri S, Triscari M, Sabatino G, Boscherini F and Sani A 2002 Fe and Mn K-edge XANES study of ancient Roman glasses *Eur. J. Mineral.* **14** 749–56

[27] Quartieri S, Riccardi M P, Messiga B and Boscherini F 2005 The ancient glass production of the Medieval Val Gargassa glasshouse: Fe and Mn XANES study *J. Non-Cryst. Solids* **351** 3013–22

[28] Capobianco N, Hunault M O J Y, Loisel C, Trichereau B, Bauchau F, Trcera N, Galoisy L and Calas G 2021 The representation of skin colour in medieval stained glasses: the role of manganese *J. Archaeol. Sci.* **38** 103082

[29] Galoisy L, Calas G and Arrio M A 2001 High-resolution XANES spectra of iron in minerals and glasses: structural information from the pre-edge region *Chem. Geol.* **174** 307–19

[30] Wilke M, Farges F, Petit P-E, Brown G E and Martin F 2001 Oxidation state and coordination of Fe in minerals: an Fe K-XANES spectroscopic study *Am. Mineral.* **86** 714–30

[31] Chalmin E, Farges F and Brown G E 2009 A pre-edge analysis of Mn K-edge XANES spectra to help determine the speciation of manganese in minerals and glasses *Contrib. Mineral. Petrol.* **157** 111–26

[32] Manceau A, Marcus M A and Grangeon S 2012 Determination of Mn valence states in mixed-valent manganates by XANES spectroscopy *Am. Mineral.* **97** 816–27

[33] Rossano S, Khomenko V, Bedidi A, Muller C, Loisel C, Ferrand J, Sarrasin L and Bertin A 2022 Glass colourations caused by Mn-Fe redox pair: application to ancient glass technology *J. Non-Cryst. Solids* **594** 121710

[34] Schalm O, Proost K, de Vis K, Cagno S, Janssens K, Mees F, Jacobs P and Caen J 2011 Manganese staining of archaeological glass: the characterization of Mn-rich inclusions in leached layers and a hypothesis of its formation *Archaeometry* **53** 103–22

[35] Tyson R and Paynter S Glass *Tintagel Revisited—New Excavations at Tintagel Castle, North Cornwall: TCARP 2016–2017* ed J A Nowakowski and J Gossip (Cornwall Council) ch 6

[36] Campbell E 1997 The early medieval imports *Whithorn and St Ninian: The Excavations of a Monastic Town 1984−91* ed P Hill (Sutton Publishing) pp 297–322

[37] Cotte M *et al* 2017 The ID21 x-ray and infrared microscopy beamline at the ESRF: status and recent applications to artistic materials *J. Anal. At. Spectrom.* **32** 477–93

[38] Ravel B and Newville M 2005 ATHENA and ARTEMIS: interactive graphical data analysis using IFEFFIT *Phys. Scr.* **2005** 1007

[39] Demšar J, Curk T, Erjavec A, Gorup C, Hocevar T, Milutinovic M, Mozina M, Polajnar M, Toplak M and Staric A 2013 Orange: data mining toolbox in python *J. Mach. Learn. Res.* **14** 2349–53

[40] Wilke M, Partzsch G M, Bernhardt R and Lattard D 2005 Determination of the iron oxidation state in basaltic glasses using XANES at the K-edge *Chem. Geol.* **220** 143–61

[41] Newville M 2013 Larch: an analysis package for XAFS and related spectroscopies *J. Phys.: Conf. Ser.* **430** 012007

[42] Solé V A, Papillon E, Cotte M, Walter P and Susini J 2007 A multiplatform code for the analysis of energy-dispersive x-ray fluorescence spectra *Spectrochim. Acta* B **62** 63–68

[43] Bidegaray A-I, Nys K, Silvestri A, Cosyns P, Meulebroeck W, Terryn H, Godet S and Ceglia A 2020 50 shades of colour: how thickness, iron redox and manganese/antimony contents influence perceived and intrinsic colour in Roman glass *Archaeol. Anthropol. Sci.* **12** 109

[44] Jackson C M, Greenfield D and Howie L A 2012 An assessment of compositional and morphological changes in model archaeological glasses in an acid burial matrix *Archaeometry* **54** 489–507

[45] Rodrigues A, Fearn S, Palomar T and Vilarigues M 2018 Early stages of surface alteration of soda-rich-silicate glasses in the museum environment *Corros. Sci.* **143** 362–75

[46] Gherardi F 2022 Compositional and morphological investigations of Roman glass from cremation deposits at Birdoswald fort on Hadrian's Wall, UK *Heritage* **5** 362–77

[47] Long B T, Peters L J and Schreiber H 1998 Solarization of soda–lime–silicate glass containing manganese *J. Non-Cryst. Solids* **239** 126–30

[48] Kunicki-Goldfinger J J 2008 Unstable historic glass: symptoms, causes, mechanisms and conservation *Stud. Conserv.* **53** 47–60

[49] Biron I and Chopinet M H 2013 Colouring, decolouring and opacifying of glass *Modern Methods for Analysing Archaeological and Historical Glass* (Wiley) pp 49–65